Amyloid Nanostructures

DOI: 10.1002/ange.200900922

Crystalline Amyloid Structures at Interfaces**

*Mathilde Lepère, Corinne Chevallard, Gerald Brezesinski, Michel Goldmann, and Patrick Guenoun**

Molecular self-assembly is now widely recognized as being able to generate ordered structures through weak (noncovalent) interactions.[1] This may take place in bulk, leading, for instance, to protein crystallization under adapted physicochemical conditions, and at interfaces as well. In the latter case, ordering can provide nanostructured interfaces useful to materials scientists to generate templates able to direct the growth of another organic or inorganic structure.[2] When biological molecules are considered, this interfacial organization can in addition be relevant to pathological or functional adsorption onto living surfaces.[3] The example of peptide interfacial self-assembly that we present in this paper shows this dual feature.

We consider here the 12 amino acid peptide LSFDNSGAITIG-NH_2 (amidated at the C terminus), referred to as LSFD, which is derived from a natural protein. LSFD was previously shown[4] to form amyloid-like fibers that are unbranched fibrils in bulk (see Figure 1) with a cross-β core structure made of self-assembled β sheets. The amyloid peptide LSFD self-assembles at a hydrophobic–hydrophilic interface like an air–water interface into flat antiparallel β sheets, thus forming a monomolecular layer.[5,6] This result demonstrates that amyloid peptides may self-assemble on surfaces, for example, on cell walls, in an organization that is quite different from that of bulk amyloid fibrils adsorbed on surfaces. This observation may provide new insights into amyloid neurodegenerative diseases.[7] Moreover, ordered β-sheet interfacial structures may be viewed as model organic surfaces for inducing the growth of minerals like calcium carbonate in biomineralization studies.[8]

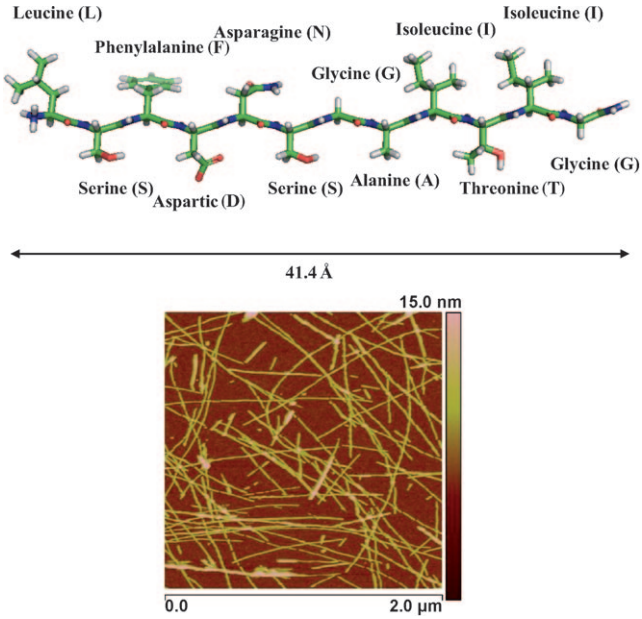

Figure 1. Top: Molecular model of the LSFD peptide in a pleated β-sheet conformation (generated with PyMol). Bottom: Amyloid fibrils formed by the LSFD peptide solubilized in ultrapure water and observed by AFM after deposition on a silicon wafer (tapping mode; topography (or height) image: the scanned area is 2 μm × 2 μm, and the thickness of the sample at any point in the scanned area is defined by the vertical color scale).

Once dissolved in a destructuring organic solvent, such as trifluoroacetic acid (TFA) mixed with chloroform (see the Experimental Section), the LSFD peptide can be spread at an air–water interface, where it organizes into a stable Langmuir film. As previously shown by infrared studies in situ,[6] an antiparallel β-sheet conformation prevails within the film all along its compression. Pressure–area isotherms evidence a first-order phase transition (see Figure 2a) near zero pressure between a "gas"-phase peptide and a condensed phase. Large-scale AFM images of films formed using TFA/$CHCl_3$ and transferred on silicon wafers (see the Experimental Section) revealed that the condensed phase is composed of elongated structures called "nanodomains" that are 5–10 Å thick, 500–1000 Å wide, and 1 μm long (see Figure 2b). The thickness ($\leq$10 Å, see Figure 2b,c) of these molecular

[*] Dr. M. Lepère, Dr. C. Chevallard, Dr. P. Guenoun
Laboratoire Interdisciplinaire sur l'Organisation Nanométrique et Supramoléculaire (LIONS)
CEA, IRAMIS, SCM
91191 Gif-sur-Yvette cedex (France)
Fax: (+33) 1-6908-6640
E-mail: patrick.guenoun@cea.fr
Homepage: http://www-drecam.cea.fr/Images/Pisp/pguenoun/pguenoun_en.html
Dr. G. Brezesinski
Max-Planck-Institut für Kolloid- und Grenzflächenforschung
Wissenschaftspark Golm
Am Mühlenberg 1, 14476 Potsdam (Germany)
Prof. M. Goldmann
Institut des Nanosciences de Paris, Campus Boucicaut
140 rue de Lourmel, 75015 Paris (France)
and
Universite Paris Descartes, UFR Biomedicale
45 rue des saints Peres, 75006 Paris (France)

[**] We acknowledge the French ACI program "Nanosciences Nanotechnologies" (project No. 0106) for financial support and the French–German Network "Complex fluids in two and a half dimensions" for sustaining French–German collaborations. We thank A. Mitraki for peptide design, J.-F. Hernandez for peptide synthesis, and N. Chevalier for his contribution to AFM imaging.

Supporting information for this article is available on the WWW under http://dx.doi.org/10.1002/anie.200900922.

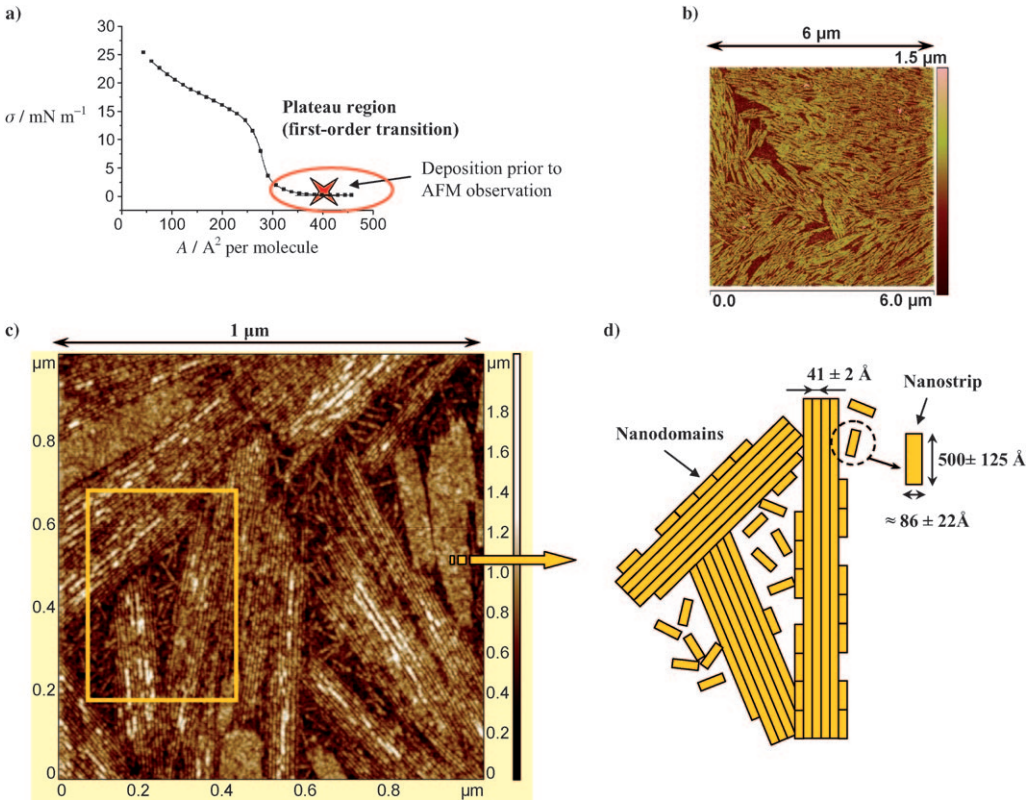

Figure 2. a) Molecular area (A)/surface pressure (σ) isotherm of the LSFD monolayer on water. The monolayer was formed from a solution of LSFD in TFA/$CHCl_3$ on the surface of deionized water. b) AFM topographic image of the LSFD peptide monolayer deposited on a silicon wafer at an average molecular area of 400 Å^2 per molecule and at zero pressure. This picture shows the existence of nanodomains 100 nm wide and about 1 µm long. c) Image of the same monolayer observed at greater magnification, revealing the fine structure of the condensed and expanded peptide phases in the coexistence region of the isotherm (zero pressure): the nanodomains exhibit a periodic structure that results from the ordered assembly of substructures called "nanostrips". Nanostrips correspond to antiparallel β sheets of finite extension that lie flat at the interface. d) Schematic representation of the coexistence of nanostrips and nanodomains.

structures makes them definitively different from bulk fibrils (ca. 100 Å thickness, see Figure 1).

Although these pictures suggest that nanodomains are made of flat β sheets that self-assemble laterally, they do not give insight to the mechanism at the nanometer scale. Figure 2c shows the transferred interfacial structures at a higher resolution. The picture clearly shows two kinds of interfacial structures coexisting at zero pressure and an average molecular area of 400 Å^2 per molecule. The condensed phase obviously corresponds to the "nanodomain" phase already observed at larger scales (Figure 2b), whereas a "gas" phase of elongated objects is observed between the nanodomains. We refer to these objects as "nanostrips" because they are of molecular thickness (5–10 Å) and about five times longer than they are wide. They are very monodisperse, and their length and width are (500 ± 125) Å and (86 ± 22) Å, respectively. The width of the nanostrips corresponds to twice the estimated length of the extended peptide backbone (41.4 Å = 12 × 3.45 Å; see Figure 1). However, given the unavoidable convolution by the AFM tip, this finding is very likely fortuitous; one cannot deduce from this single measurement that a nanostrip consists of two individual β sheets associated side-by-side.

As shown in Figure 2c, the nanodomains do not exhibit well-defined edges, but rather grow through nanostrip aggregation. Thus, the first-order transition detected on isotherms arises from the self-assembly of these nanostrips into ordered aggregates that build up the nanodomains.

To complement AFM on transferred Langmuir–Blodgett films and to provide more comprehensive average views of the in situ layers, surface X-ray diffraction experiments were carried out at HASYLAB (DESY, Hamburg, Germany) on the BW1 beamline (see the Experimental Section) Figure 3 presents the typical series of Bragg peaks obtained on the acidic subphase (TFA/$CHCl_3$ solvent) along the compression isotherm. These peaks can be indexed using a rectangular unit cell with the parameters a and b. This unit cell contains two molecules. Parameter a (9.62 Å in Figure 3) expresses the antiparallel β-sheet ordering of the LSFD peptide at the interface. The (20) peak therefore corresponds to a repeat distance of 4.81 Å, which is the typical interstrand distance defined by the hydrogen-bond network in a β-sheet conformation (Figure 3c). The intensity and position of this peak does not vary during the compression of the film. The absence of the (10) peak can be a consequence of a null unit-cell form factor as a result of the identity between the electronic density of the two molecules in the unit cell.[9]

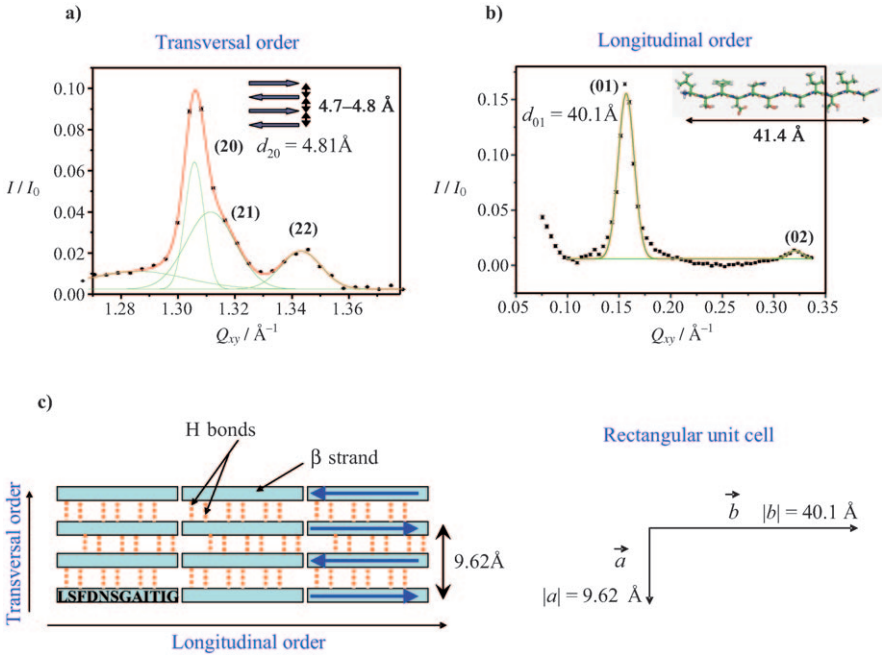

Figure 3. Bragg peaks observed in GIXD experiments at the air/water interface of the LSFD monolayer (formed from a TFA/$CHCl_3$ solution) at $\pi = 6.3$ mN m^{-1}. The peak indexing uses a rectangular unit cell with parameters $a = 9.62$ Å and $b = 40.1$ Å. a) Bragg peak (20) corresponding to peptide ordering along the hydrogen-bond direction ("transversal" order). Diagonal peaks (21) and (22) are also visible, confirming the existence of a 2D crystalline order. b) Bragg peaks related to the "longitudinal" order, along the peptide backbone. c) Sketch of the transversal and longitudinal orders and unit cell used to index the Bragg peaks.

Another series of peaks at lower Q_{xy} is associated with peptide ordering along the peptidic backbone with a repeat distance $b = 40.1$ Å at $\pi = 6.3$ mN m^{-1}, which nicely coincides with the length of the peptide in a fully extended configuration (Figure 3b). The longitudinal repeat distance b hardly varies with the surface pressure, decreasing from 42 Å at zero pressure to 39 Å at 15 mN m^{-1} (see Figure S1 in the Supporting Information). The longitudinal peaks, indexed (01) and (02), exhibit an out-of-plane component, with a maximum intensity at $Q_z = 0.3236$ Å^{-1} determined on the peak (01) whose full-width at half-maximum (fwhm) allows an estimation of the film thickness L_z: $L_z = 0.9 \times 2\pi/\text{fwhm}(Q_z) = 0.9 \times 2\pi/0.6 = 9.42$ Å (see Figure S2 in the Supporting Information). This value is in full agreement with a flat β-sheet monolayer thickness and with the thicknesses determined by AFM. The out-of-plane component of the peak points toward a longitudinal tilt of the molecules, with an estimated tilt angle of about 26° between the peptide backbone and the water surface. Alternatively, it may be induced by a modulation of the electronic density along the z axis of the molecule. A close investigation of this aspect is under progress.

The existence of two series of peaks points to two-dimensional crystalline order of the LSFD peptide at the interface, both along the hydrogen-bond network ("transversal" order) and along the peptidic backbone ("longitudinal" order). This 2D order is confirmed by the presence of two other peaks (1.313 Å^{-1} and 1.344 Å^{-1}) identified as diagonal peaks (21) (expected at 1.315 Å^{-1}) and (22) (expected at 1.343 Å^{-1}) (Figure 3). Thus, the first-order transition consists of the appearance and growth of a new phase, the nanodomain phase evidenced by AFM observations, which is characterized by a crystalline longitudinal order absent of the 1D crystalline nanostrip phase. The longitudinal repeat distance deduced from X-ray studies agrees very well with the structure periodicity extracted by processing the AFM images (41 ± 2 Å), despite potential perturbations resulting from film transfer. Nanostrips, which can be viewed as amphipathic β sheets, order side-by-side in the course of the transition to form nanodomains, and generate the longitudinal order resulting in the (01) peak.

Using Scherrer's formula,[10] the in-plane coherence lengths in the two crystalline directions (peaks (20) and (01)) can be estimated. The transversal coherence length amounts to about 700 Å (resolution-limited) all along the compression. This means that both isolated nanostrips and nanodomains involve crystallites of more than 150 transversally ordered peptides. The longitudinal coherence length, also constant along the compression, is estimated to be about 300 Å (about nine nanostrips).

Whereas the TFA/$CHCl_3$ solvent provides very acidic conditions (pH 2.6) arising from TFA dissolution in the water subphase and resulting in fully protonated aspartic acid groups, the hexafluoroisopropanol (HFIP)/$CHCl_3$ solvent system induces a partial ionization of these groups (pH 5.5). Changing the conditions for the formation of the LSFD film does not modify the periodicity and the apparent coherence length of the transversal order but does affect the longitudinal order. The latter is weakened in the case of a neutral subphase (HFIP/$CHCl_3$ solvent system) where the longitudinal coherence length drops down to 250 Å. The repeat distance obtained by X-ray diffraction (105 Å) is in excellent agreement with an AFM periodicity of 120 Å (Figure 4a). In contrast to the TFA case, these values point to a nanostrip width defined by the end-to-end association of at least two peptides. The addition of 10 mM $CaCl_2$ to the subphase leads to a very strong longitudinal order with five diffraction orders visible (Figure 5) and a restored coherence length as large as in the TFA case. The two detectable peaks of lowest order are, as in the absence of salt, the (02) and (03) peaks (Figure 5). The repeat distance is twice that observed under acidic conditions (88 Å), again in excellent agreement with the periodicity of 82 Å found by AFM (Figure 4b). This likely means that the unit cell now contains four molecules when HFIP is used as a solvent. This paves the way for future experiments on calcium carbonate mineralization under well-ordered templates.

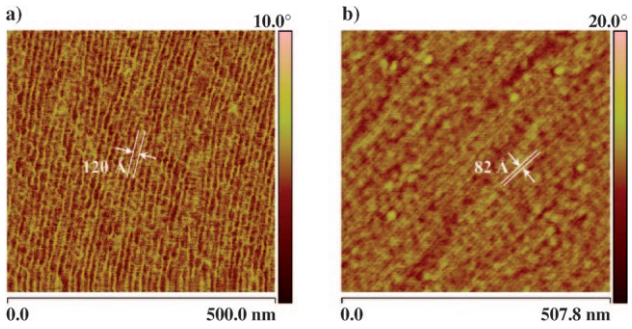

Figure 4. AFM phase images (tapping mode) of LSFD monolayers formed under two different conditions but at the same spreading pressure ($\pi = 0.2$ mN m^{-1}) prior to transfer on silicon wafer: a) monolayer formed from an HFIP/$CHCl_3$ solution on a deionized water subphase; b) monolayer formed from an HFIP/$CHCl_3$ solution on a 10 mM $CaCl_2$ subphase. Both images show a regular arrangement of long structures, which are β-sheet structures (nanostrips), as highlighted by GIXD studies. The observed periodic structure results from the longitudinal assembly of the nanostrips. In both images, processing by fast Fourier transform indicates a spatial periodicity with a value of 120 Å for the pure water subphase and 82 Å for the $CaCl_2$ subphase.

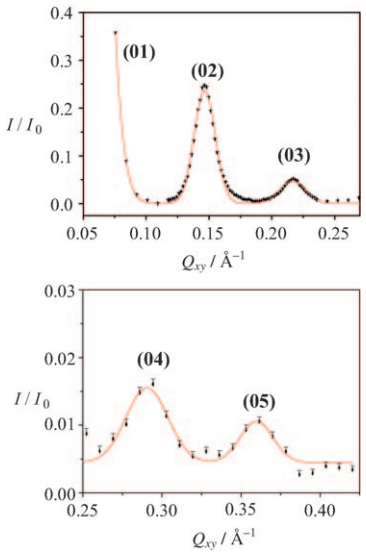

Figure 5. Plot of scattered intensity I (normalized to the incoming intensity I_0) versus the in-plane component Q_{xy} of the scattering vector **Q** for an LSFD monolayer formed from an HFIP/$CHCl_3$ solution at the surface of a 10 mM $CaCl_2$ subphase and compressed to $\pi = 15$ mN m^{-1}. Five Bragg peaks corresponding to the longitudinal order are observed.

We described herein the detailed characterization of the interfacial organization of the LSFD peptide by AFM measurements and X-ray surface crystallography, which nicely complement and agree with each other. We demonstrated how a 2D crystalline order progressively builds up in response to the increased packing density of the peptide at the air–water interface. The interfacial amyloid structures differ completely from their bulk counterparts. In nature, such structures may determine the functionalities of the surface as in the case of microorganisms where they seem to design a functional hydrophobic coat favoring adhesion or dispersion in air.[11]

Experimental Section

Peptides: The LSFD peptide used in this study was obtained from Eurogentec (France) as the trifluoroacetate salt or synthesized in our laboratory according to the procedure described in Ref. [6]. Both batches provided similar results.

Peptide solutions: Lyophilized peptides were dissolved in trifluoroacetic acid (TFA) or hexafluoroisopropanol (HFIP) at concentrations of 0.7 and 0.98 mg mL^{-1}, respectively, and then diluted with chloroform to a final concentration of 0.07 mg mL^{-1} for the TFA/$CHCl_3$ (1:9) solvent system, and 0.14 mg mL^{-1} for the 1:6 HFIP/$CHCl_3$ (1:6) solvent system.

Film formation: Peptide films at the air–water interface were prepared in a two-barrier Langmuir trough (Riegler & Kirstein, Potsdam, Germany) equipped with a Wilhelmy balance. The peptide solution was first spread onto the free surface of the aqueous subphase in the trough, either an ultrapure water subphase (18.2 MΩ cm, pH 5.8) or 10 mM $CaCl_2$ solution. Then, the film was compressed at a constant rate of 0.62 Å^2(residue·min) to the target surface pressure.

Atomic force microscopy: The peptide film was transferred onto a silicon wafer by vertical Langmuir–Blodgett deposition at different surface pressure values. In all cases, the transfer ratio was 100%. Atomic force microscopy (AFM) images were recorded using a Nanoscope 3100 Instrument or a M5 Parks Instrument (Veeco) in tapping mode.

GIXD experiments: Grazing incidence X-ray diffraction measurements on the peptide monolayers were carried out at HASYLAB (Hamburg, Germany) using the BW1 beam line of the DESY synchrotron source.[12] The monochromatic X-ray beam ($\lambda = 1.304$ Å) was adjusted to strike the air–water interface at the grazing incidence angle $\alpha_i = 0.85\ \alpha_c$, where α_c (0.13°) is the critical angle for total reflection of the X-ray beam at the water surface. GIXD diffraction signals result from the existence of peptide ordered domains at the air–water interface. The scattered intensity was detected by a linear position-sensitive detector (PSD, OEM-100M, Braun, Garching, Germany). The out-of-plane Q_z component of the scattering vector was detected in the range $0\ \text{Å}^{-1} \le Q_z \le 1\ \text{Å}^{-1}$. The accumulated position-resolved counts were not corrected for polarization, effective area, and Lorentz factor as we were only interested in determining the peak positions. Model peaks, taken as Gaussian in both the in-plane and the out-of-plane directions, fitted by the least-squares method to the measured intensities. The diffraction data consisted of Bragg peaks at diagnostic Q_{xy} values. To access the extent of the crystalline order in the monolayer, the in-plane coherence length L_{xy} was approximated from the full width at half maximum (fwhm) of the Bragg peaks using $L_{xy} \approx 0.9(2\pi)/\text{fwhm}(Q_{xy})$. The diffracted intensity normal to the interface was integrated over the Q_{xy} window containing the diffraction peak to calculate the corresponding Bragg rod. The thickness of the monolayer was estimated from the fwhm of the Bragg rod using $0.9(2\pi)/\text{fwhm}(Q_z)$.

Received: February 16, 2009
Published online: May 28, 2009

Keywords: nanostructures · peptides · self-assembly · surfaces

[1] G. Whitesides, M. Boncheva, *Proc. Natl. Acad. Sci. USA* **2002**, *99*, 4769–4774.
[2] a) S. Cavalli, D. Popescu, E. E. Tellers, M. R. J. Vos, B. P. Pichon, M. Overhand, H. Rapaport, N. Sommerdijk, A. Kros, *Angew. Chem.* **2006**, *118*, 753–758; *Angew. Chem. Int. Ed.* **2006**, *45*, 739–

744; b) J. Aizenberg, D. A. Muller, J. L. Grazul, D. R. Hamann, *Science* **2003**, *299*, 1205 – 1208.
[3] M. F. B. G. Gebbink, D. Claessen, B. Bouma, L. Dijkhuizen, H. A. B. Wöste, *Nat. Rev. Microbiol.* **2005**, *3*, 333 – 341.
[4] M. Luckey, J.-F. Hernandez, G. Arlaud, V. T. Forsyth, R. W. H. Ruigrok, A. Mitraki, *FEBS Lett.* **2000**, *468*, 23 – 27.
[5] M. Lepère, A. H. Muenter, C. Chevallard, P. Guenoun, G. Brezesinski, *Colloids Surf. A* **2007**, *303*, 73 – 78.
[6] M. Lepère, C. Chevallard, J.-F. Hernandez, A. Mitraki, P. Guenoun, *Langmuir* **2007**, *23*, 8150 – 8155.
[7] a) J. McLaurin, A. Chakrabartty, *J. Biol. Chem.* **1996**, *271*, 26482 – 26489; b) M. Boqvist, F. Lindstrom, A. Watts, G. Grobner, *J. Biol. Chem.* **2004**, *335*, 1039 – 1049.
[8] a) S. Mann in *Biomineralization: Principles and Concepts in Bioinorganic Materials Chemistry*, Oxford University Press, New York, **2001**; b) H. A. Lowenstam, S. Weiner in *On Biomineralization*, Oxford University Press, New York, **1989**.
[9] J. Daillant, M. Alba, *Rep. Prog. Phys.* **2000**, *63*, 1725 – 1777.
[10] A. Guinier in *X-Ray Crystallographic Technology*, Hilger and Watts, London, **1952**, pp. 235 – 237.
[11] a) M. Chapman, L. Robinson, J. Pinkner, R. Roth, J. Heuser, M. Hammar, S. Normark, S. Hultgren, *Science* **2002**, *295*, 851 – 855; b) H. Wosten, M. Richter, J. Willey, *Fungal Genet. Biol.* **1999**, *27*, 153 – 160.
[12] a) J. Als-Nielsen, D. Jaquemain, K. Kjaer, M. Lahav, F. Levellier, L. Leiserowitz, *Phys. Rep.* **1994**, *246*, 251 – 313; b) K. Kjaer, *Physica B* **1994**, *198*, 100 – 109; c) R. Rietz, W. Rettig, G. Brezesinski, W. G. Bouwman, K. Kjaer, H. Möhwald, *Thin Solid Films* **1996**, *285*, 211 – 215.

